J Gynecol Oncol. 2020 May;31(3):e28
https://doi.org/10.3802/jgo.2020.31.e28
pISSN 2005-0380·eISSN 2005-0399

JOURNAL OF GYNECOLOGIC ONCOLOGY

Original Article

Quantitative analysis of proteins related to chemoresistance to paclitaxel and carboplatin in human SiHa cervical cancer cells via iTRAQ

Yue He, Su-Bin Han, Yu-Ning Geng, Shu-Li Yang, Yu-Mei Wu

Department of Gynecological Oncology, Beijing Obstetrics and Gynecology Hospital, Capital Medical University, Beijing, China

Received: Feb 12, 2019
Revised: Sep 24, 2019
Accepted: Oct 16, 2019

Correspondence to
Yu-Mei Wu
Department of Gynecological Oncology, Beijing Obstetrics and Gynecology Hospital, Capital Medical University, Dongcheng District, Qi-he-lou street No.17, Beijing 100006, China.
E-mail: wym597118@163.com

ORCID iDs
Yue He
https://orcid.org/0000-0003-4041-9271
Su-Bin Han
https://orcid.org/0000-0002-5264-564X
Yu-Ning Geng
https://orcid.org/0000-0001-5800-992X
Shu-Li Yang
https://orcid.org/0000-0003-2128-1836
Yu-Mei Wu
https://orcid.org/0000-0002-2242-9348

ABSTRACT

Objective: This study aimed to identify proteins related to paclitaxel and carboplatin chemoresistance in cervical cancer.
Methods: Quantitative proteomic analysis was performed on normal SiHa cells and those treated with paclitaxel and carboplatin for 14 days, with isobaric tags for relative and absolute quantitation (iTRAQ) analysis. Gene Ontology (GO) and Kyoto Encyclopedia of Genes and Genomes (KEGG) enrichment analyses were used to identify related processes and differentially expressed proteins.
Results: A total of 67 and 96 differentially expressed proteins were identified in the paclitaxel- and carboplatin- treated groups, respectively. GO and KEGG enrichment analyses identified 53 (43 upregulated and 10 downregulated) and 85 differentially expressed proteins (70 upregulated and 15 downregulated) in the paclitaxel- and carboplatin-treated groups, respectively. The cell counting kit-8 results revealed that APOA1 was overexpressed in both the paclitaxel- and carboplatin- resistant SiHa cells compared with the control cells. Immunohistochemistry showed that APOA1 was highly expressed in the paclitaxel- and carboplatin- resistant squamous cell carcinoma of the cervix.
Conclusion: This study is the first to use iTRAQ to identify paclitaxel- and carboplatin-resistance proteins in cervical cells. We identified several proteins previously unassociated with paclitaxel and carboplatin resistance in cervical cancer, thereby expanding our understanding of paclitaxel and carboplatin resistance mechanisms. Moreover, these findings indicate that the APOA1 protein could serve as a potential marker for monitoring and predicting paclitaxel and carboplatin resistance levels.

Keywords: Antineoplastic Agent Resistance; Paclitaxel; Carboplatin; Cervical Cancer; Protein Microarray Analysis

INTRODUCTION

Cervical cancer is the fourth most common cancer in women worldwide, with an estimated 528,000 new cases and 266,000 deaths in 2012 [1]. Most cervical cancer cases (84% or 445,000 cases) and deaths (87% or 230,000 cases) occur in less developed regions [1]. In addition to a higher incidence of cervical cancer, the patients living in these areas have a

Funding

Funding was gratefully received from the Beijing Municipal Science and Technology Commission (grant No. D131100005313009); Capital's Funds for Health Improvement and Research (grant No. 2018-4-2113); Beijing Obstetrics and Gynecology Hospital, Capital Medical University (grant No. fcyy201601); Beijing Municipal Administration of Hospitals Clinical Medicine Development of Special Funding Support (grant No. ZYLX201705); Scientific Research Common Program of Beijing Municipal Commission of Education (KM201910025006).

Conflict of Interest

No potential conflict of interest relevant to this article was reported.

Author Contributions

Conceptualization: H.Y., G.Y.N., W.Y.M.; Data curation: H.Y., W.Y.M.; Formal analysis: H.Y., Y.S.L.; Funding acquisition: H.Y., W.Y.M.; Investigation: H.S.B., G.Y.N.; Methodology: H.S.B., Y.S.L.; Project administration: W.Y.M.; Resources: G.Y.N., Y.S.L.; Supervision: W.Y.M.; Writing - original draft: H.Y.; Writing - review & editing: W.Y.M.

higher rate of locally-advanced stages, including stages IB2 and IIA2 as classified by the International Federation of Gynecology and Obstetrics in 2009 year [2]. This is partly due to the lack of coordinated screening programs and/or lack of access to radiotherapy, which leads to lower overall survival. Thus, novel methods are required to improve the treatment outcomes of advanced or locally-advanced cervical cancer (LACC).

Concurrent chemoradiation therapy (CCRT) is a standard treatment for patients with LACC, which has a 5-year overall survival rate of approximately 60%–65% [3]. However, local and distant recurrences (17% and 18%, respectively) of LACC after CCRT are still encountered [4]. The chemotherapies developed to improve treatment outcomes of cervical cancer which including neoadjuvant chemotherapy (NACT) before CCRT and radical hysterectomy [5]. The aim of NACT is improve the prognosis of patients with LACC by shrinking the tumor and killing metastatic cells before further treatment; however, there is currently no standard NACT regimen [6]. The safety of paclitaxel plus carboplatin as a NACT has been demonstrated in many studies [7], with its efficacy against cervical squamous cell carcinoma varying from patient to patient. The prognosis for NACT-sensitive patients with tumor regression is good; however, it is poor for NACT-resistant patients. This study aimed to identify proteins related to paclitaxel and carboplatin chemoresistance in cervical cancer to provide a basis for future studies on chemoresistance mechanisms.

MATERIALS AND METHODS

1. Cell lines

SiHa cells were purchased from the American Type Culture Collection (ATCC, Manassas, VA, USA) and cultured in Dulbecco's Modified Eagle Medium supplemented with 10% fetal bovine serum (Sigma, St. Louis, MO, USA) and 1% penicillin/streptomycin (HyClone, Logan, UT, USA) at 37°C with 5% CO_2. The cell line was subjected to short tandem repeat (STR) classification identification, as recommended by the ATCC.

2. Cell cytotoxicity and cell count assay

We used cell counting kit-8 (CCK-8) assays to assess cell viability. Cells were seeded onto 96-well plates at a density of 2×10^3 cells/well, then 10 μL of CCK-8 solution was added to each well at the indicated time. After incubation for 4 hours at 37°C in a humidified atmosphere containing 5% CO_2, the optical density (OD) was recorded at 450 nm using a microplate reader (Bio-Rad, Richmond, VA, USA). These experiments were performed in triplicate.

Cells were plated onto 96-well plates (Corning 3599; Sigma) at 20% confluency, then treated with paclitaxel and carboplatin. When the control cells had reached approximately 80% confluence, the cells were counted using a cell counter (Nexcelom, Lawrence, MA, USA) a minimum of 4 times for each treatment.

3. Protein sample preparation and isobaric tags for relative and absolute quantitation (iTRAQ) labeling

Paclitaxel- and carboplatin- treated cells and untreated cells were grown to 80% confluence over 14 days in Corning T-25 flasks. After 14 days of co-culture, the cells were washed with phosphate-buffered saline, collected by incubation with 2 mL cellular lysis buffer (8M urea, 2% CHAPS, and 1M DTT), and processed ultrasonically (Sonifier cell disruptor; 50 W for 30 seconds; Heat Systems-Ultrasonics Inc., Plainview, LI, USA). After centrifugation at 14,000×g

JOURNAL OF GYNECOLOGIC ONCOLOGY

for 15 minutes, the cells were lysed and passed through a 0.45 mm filter to remove insoluble particles, then stored at −80°C until further use. The protein density of the cellular lysis buffer was determined to allow the concentrations to be adjusted to identical levels. For each sample, 100 μg of protein was mixed with acetone and precipitated overnight at −20°C, dissolved in lysis buffer, denatured, and then cysteines were blocked as described in the iTRAQ protocol (Applied Biosystems, Framingham, MA, USA). Each sample was digested with 20 mL trypsin solution (AB Sciex, Ontario, Canada) at 37°C overnight and labeled with iTRAQ tags as follows: the mock (normal SiHa cell) group was labeled with the 116 tag; the paclitaxel group was labeled with the 117 tag; and the carboplatin group was labeled with the 121 tag.

4. EASY liquid chromatography–electrospray ionization–tandem mass spectrometry (EASY nLC-MS/MS)

To reduce sample complexity during EASY nLC-MS/MS analysis, the sample pools were diluted 10-fold with SCX buffer (ICAT Cation Exchange Buffer Pack) and processed using the Acclaim PepMap RSLC (50 μm×15 cm, nano viper, P/N164943; Thermo Scientific, Waltham, MA, USA). The peptide samples were analyzed by EASY nLC MS/MS using the Q Exactive Plus system interfaced with the EASY-nLCsystem (Thermo Scientific). The chromatographic capillary columns were packed with X Bridge Peptide BEH C18 Column (Waters Co., Milford, MA, USA) and reversed phase material in 100% acetonitrile (ACN) at a pressure of 1,000 per square inch (Thermo Scientific) and a flow rate of 3 mL/min, and separated using an analytical Acclaim PepMap RSLC. The peptide samples of each SCX fraction were enriched using an Acclaim PepMap column (RSLC, 50 μm×15 cm, nano viper, P/N164943; Thermo Scientific) at a flow rate of 300 nL/min. The peptides were eluted using a linear gradient of 2%–80% ACN over 180 minutes and MS analysis was performed with full scans in a data-dependent manner using the Q Exactive Plus mass analyzer at a mass resolution of 70,000 and 350–1,800 m/z. For each MS cycle, the 10 highest intensity precursor ions from a survey scan were selected for MS/MS.

5. Data processing, protein identification, and statistical analyses

The data of MS/MS spectra were analyzed by using Mascot software (version 2.5; Matrix Science, Boston UK) (database: Uniprot_HomoSapiens_159615_20170811) [8]. Confidence values were calculated for each peptide according to the agreement between the experimental and theoretical fragmentation patterns. For protein identification and quantification, a peptide mass tolerance of 20 ppm was permitted for intact peptide masses, and 0.1 Da for fragmented ions. Each protein was assigned a confidence score (0%–100%) based on their unique spectral patterns; those with confidence scores >90% (at least 1 peptide had 95% identification confidence) were used for further quality control and differential expression analyses. If all the identified peptides had ion scores above the Mascot peptide identity threshold, a protein was considered identified if it displayed at least 1 unique peptide match. To identify significant changes in the protein-abundance ratios measured using iTRAQ, a 1.2-fold change and false discovery rate (FDR) <0.05 were used as thresholds.

6. Functional enrichment analysis

Theoretical pI values and molecular weights (MWs) of the identified proteins were obtained from the UniProt protein sequence database. Functional enrichment analysis was performed using Gene Ontology (GO) (http://geneontology.org/). GO annotation was used to describe the functions of the differentially expressed proteins, which were classified into 3 major categories: cellular component, molecular function, and biological process [9]. Pathway analysis was performed by Kyoto Encyclopedia of Genes and Genomes (KEGG) mapping. Both analyses identified significant differences with $p<0.01$ and $p<0.05$, respectively.

https://doi.org/10.3802/jgo.2020.31.e28

JOURNAL OF GYNECOLOGIC ONCOLOGY

7. Polymerase chain reaction (PCR) verification of lentivirus-mediated APOA1 overexpression

The GO and KEGG enrichment analyses identified the APOA1 protein as relating to paclitaxel and carboplatin resistance. An APOA1-overexpression lentivirus with puromycin was constructed by GeneChem (Shanghai, China). Puromycin was added to the medium to screen infected cells, and the experiment was allowed to continue when the APOA1 lentivirus infection efficiency was >70%.

APOA1-overexpressing SiHa cells were homogenized, then their total RNA was extracted with Trizol reagent (Invitrogen Life Technologies, Carlsbad, CA, USA) and quantified by ultraviolet spectroscopy. Reverse transcription (RT) was performed in a 20 mL reaction system with 4 mg of total RNA treated by RNase-free DNase I (Takara BIO, Otsu, Japan), according to the manufacturer's instructions. The following PCR primers were purchased from Takara BIO: GAPDH, forward 5′-TGACTTCAACAGCGACACCCA-3′ and reverse 5′-CACCCTGTTGCTGTAGCCAAA-3′; APOA1 forward 5′-CCCTGGGATCGAGTGAA GGA-3′ and reverse 5′-CTGGGACACATAGTCTCTGCC-3′. Quantitative RT-PCR was performed using the Thermal Cycler Dice Real Time System (TP800; Takara, Kusatsu, Japan). The relative target gene mRNA expression data were quantified using the $2^{-\Delta\Delta Ct}$ method, where Ct was the cycle threshold.

8. Verification of APOA1 expression in squamous cell cervical tissues by immunohistochemistry (IHC) and western blotting (WB)

Cervical squamous cell carcinoma tissue samples were collected from ten patients who visited the Beijing Obstetrics and Gynecology Hospital, Capital Medical University between January 1, 2017, and June 1, 2017. Tissue pathology was confirmed by 2 chief pathologists at the hospital, and samples were stored at −80°C.

Clinical remission was evaluated according to World Health Organization Response Evaluation Criteria in Solid Tumors (RECIST) [10]. The complete response (CR) is defined as disappearance of all target lesions. Any pathological lymph nodes (whether target or nontarget) must have reduction in the short axis to <10 mm. The partial remission (PR) is defined as at least 30% decrease in the sum of diameters of target lesions, taking as reference the baseline sum diameters. The progressive disease (PD) is defined as at least 20% increase in the sum of diameters of target lesions, taking as reference the smallest sum on study (including the baseline sum if that is the smallest on study). In addition, the relative increase of more or new lesion is also considered as progression. The stable disease (SD) is defined as neither sufficient shrinkage to qualify for PR nor sufficient increase to qualify for PD, in reference to the smallest sum diameters during the study. Computed tomography (CT) and magnetic resonance imaging (MRI) are the best currently available and reproducible method to measure lesions selected for response assessment. This guideline has defined measurability of lesions on CT scan based on the assumption that CT slice thickness is 5 mm or less, when CT scans have slice thickness greater than 5 mm, the minimum size for a measurable lesion should be twice the slice thickness. MRI is also acceptable in certain situations. If the 2 oncologists reached different conclusions, the results were rechecked by 2 radiologists and a third oncologist was invited to discussion until a consensus was reached.

The immunohistochemical staining results were assigned a mean score considering both the staining intensity and the proportion of tumor cells with an unequivocal positive reaction. Each section was assessed independently by 2 pathologists without prior knowledge of patient data. Positive reactions were defined as those with brown signals visible in the cell

https://doi.org/10.3802/jgo.2020.31.e28

cytoplasm. A staining index (0–12) was determined by multiplying the staining intensity score with the positive area score. Intensity was scored as follows: 0, negative; 1, weak; 2, moderate; and 3, strong. Positive cell frequency was defined as follows: 0, <5%; 1, 5%–25%; 2, 26%–50%; 3, 51%–75%, and 4, >75%. For statistical analysis: scores between 0 and 7 were considered low, whilst scores between 8 and 12 were considered high.

The tissues (20 mg) were lysed and centrifuged, and the supernatant was collected. Protein concentration was determined using bicinchoninic acid (Pierce, Waltham, MA, USA). Electrophoresis was carried out in 10% separating gel at 70 V and 4% stacking gel at 100 V, then the proteins were transferred to a polyvinylidene fluoride membrane for 60 minutes. The membrane was blocked in 5% non-fat milk for 1 hour at 25°C and incubated with primary antibodies (DDDDK tag antibody; Proteintech, Rosemont, IL, USA) at a ratio of 1:2,000 at 4°C overnight. Next, the membrane was incubated with secondary antibodies (anti-rabbit secondary antibody; Proteintech) at a ratio of 1:2,000 for 1 hour at 25°C and protein bands were visualized using an Amersham lmager 600. The clearest bands were scanned into a computer for semi-quantification; the OD of each band was determined using IMAGE J software and was normalized to that of β-actin (Proteintech).

9. Statistical analysis

The half-maximal inhibitory concentration (IC_{50}) was used to evaluate the relationship between the carboplatin and paclitaxel concentrations and cell survival, and was calculated using GraphPad Prism5 Software (GraphPad Software Inc., San Diego, CA, USA). GO and KEGG mapping pathway enrichment were evaluated using 2-sided Fisher's exact tests ($p<0.05$). All statistical analyses were performed using SAS 9.3 software (SAS institute, Cary, NC, USA). Each experiment was repeated 3 times.

RESULTS

1. Determination of paclitaxel and carboplatin concentrations

We evaluated the optimal concentrations of paclitaxel and carboplatin for treating SiHa cells, which were found to be 8.789 ng/mL and 14.19 μg/mL, respectively, using a semi-logarithmic plot (**Fig. 1A and C**). We also determined the concentrations required to inhibit the growth of the SiHa cells by adding different concentrations of paclitaxel (S1215; Selleck, Houston, TX, USA; 0, 0.0007873, 0.001563, 0.003125, 0.00625, 0.0125, 0.025, 0.05, 0.1, and 0.2 μg/mL) and carboplatin (S1215; Selleck; 0, 5.85, 8.78, 13.17, 19.75, 29.63, 44.44, 66.67, 100, and 150 μg/mL) to the culture solution. The inhibitory paclitaxel and carboplatin concentrations were selected according to the level of cell inhibition after 14 days of culture. Paclitaxel concentrations of 0.002 and 0.004 μg/ml inhibited cell growth by 23.34% and 74.12%, respectively; therefore, a concentration of 0.003 μg/ml was selected for further experiments (**Fig. 1B**). A carboplatin concentration of 0.2 μg/mL inhibited cell growth by 35.47% after 14 days of culture (**Fig. 1D**); therefore, this concentration was used for further experiments.

2. Mass spectrometry, protein identification, and quantitative analysis

Proteins were extracted from cultured SiHa cells and quantified using the Bradford assay according to the manufacturer's instructions. A total of 7,139 proteins were identified according to the Swiss-Prot human library, with 85,151 peptide segments displaying an FDR of < 1% (**Supplementary Table 1**).

https://doi.org/10.3802/jgo.2020.31.e28

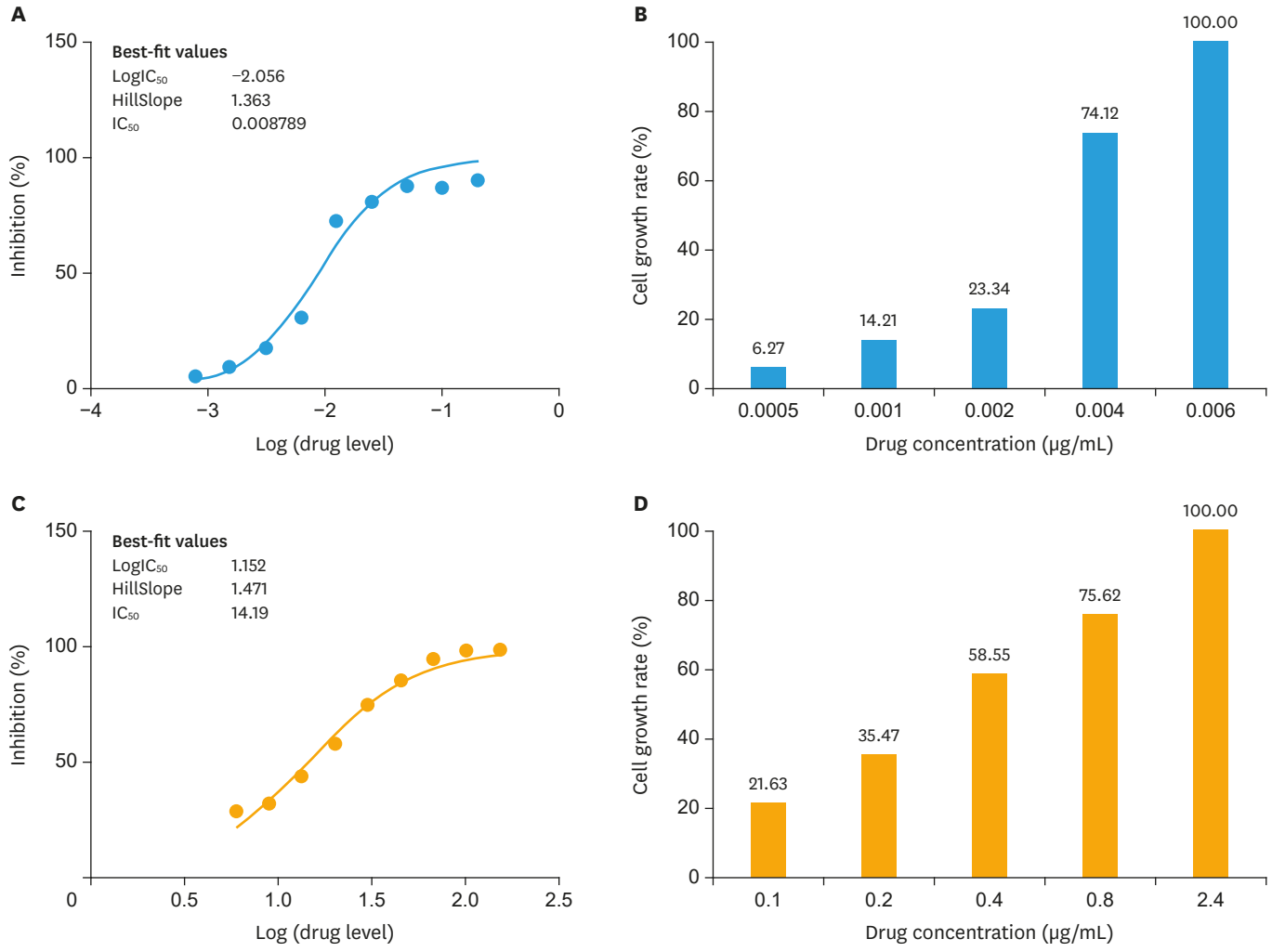

Fig. 1. (A, B) Dose response to PTX. (C, D) Dose response to CBP. (A) The IC_{50} of PTX was calculated as 8.789 ng/mL; (B) When the drug concentration was 0.002 μg/mL, the inhibition rate of cell growth rate was 23.34% after 14 days of culture. When the drug concentration was 0.004 μg/mL, the inhibition rate of cell growth rate was 74.12% after 14 days of culture. The concentration of 0.003 μg/mL was used for further experiments; (C) The IC_{50} of CBP was 14.19 μg/mL; (D) When treated with 0.2 μg/mL of carboplatin, cell growth was inhibited by 35.47% after 14 days of culture. This concentration was used for further experiments.
CBP, carboplatin; IC_{50}, half-maximal inhibitory concentration; PTX, paclitaxel.

3. Data processing, protein identification, and statistical analyses

All 7,139 proteins were labeled by iTRAQ and identified by EASY nLC-MS/MS. Low molecular weight proteins (1,000–50,000 Da) were selected as putative biomarkers and screened by comparatively analyzing their protein expression in the paclitaxel- and carboplatin-treated groups. The screening criteria were expression levels of >1.2-fold for the upregulated proteins and <0.83-fold for the downregulated proteins. The retrieval of related protein functions from the literature allowed 67 different paclitaxel protein peaks and 96 different carboplatin peaks to be identified and selected.

4. GO and KEGG pathway analyses

We identified the functions and pathways of the target proteins by performing GO and KEGG pathway analyses; the significantly differentially expressed proteins were selected and confirmed via enrichment analysis. In the paclitaxel vs. mock group there were 53 differentially expressed proteins, 43 upregulated and 10 downregulated (**Fig. 2**). Furthermore,

https://doi.org/10.3802/jgo.2020.31.e28

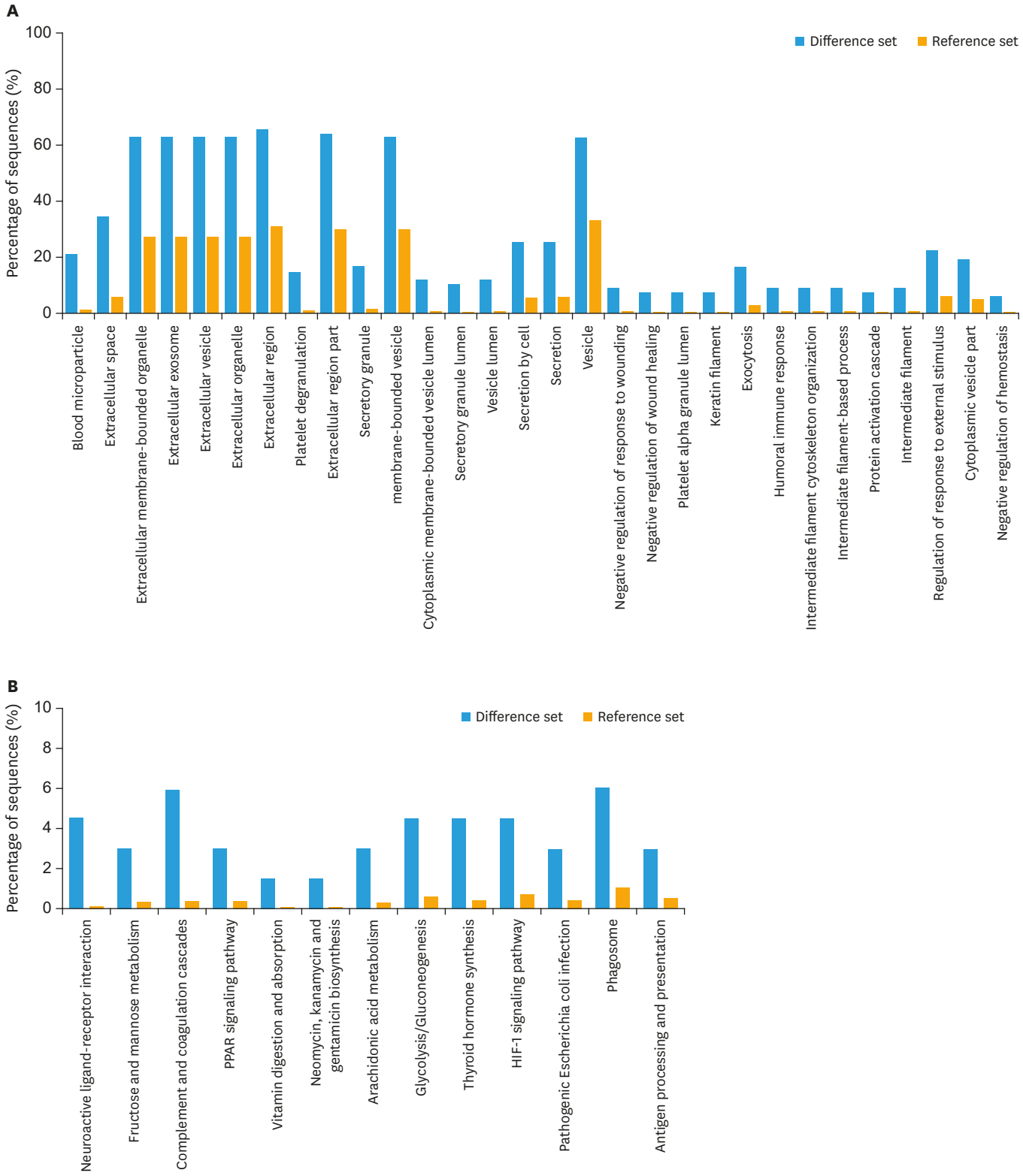

Fig. 2. GO and KEGG analysis in paclitaxel group. (A) GO enrichment analysis in the paclitaxel vs. mock group (top 30); (B) KEGG pathway analysis in the paclitaxel vs. mock group.
GO, Gene Ontology; KEGG, Kyoto Encyclopedia of Genes and Genomes.

https://doi.org/10.3802/jgo.2020.31.e28

in the carboplatin vs. mock group there were 85 differentially expressed proteins, 70 upregulated and 15 downregulated (**Fig. 3**). Of these, 5 of the proteins upregulated in the

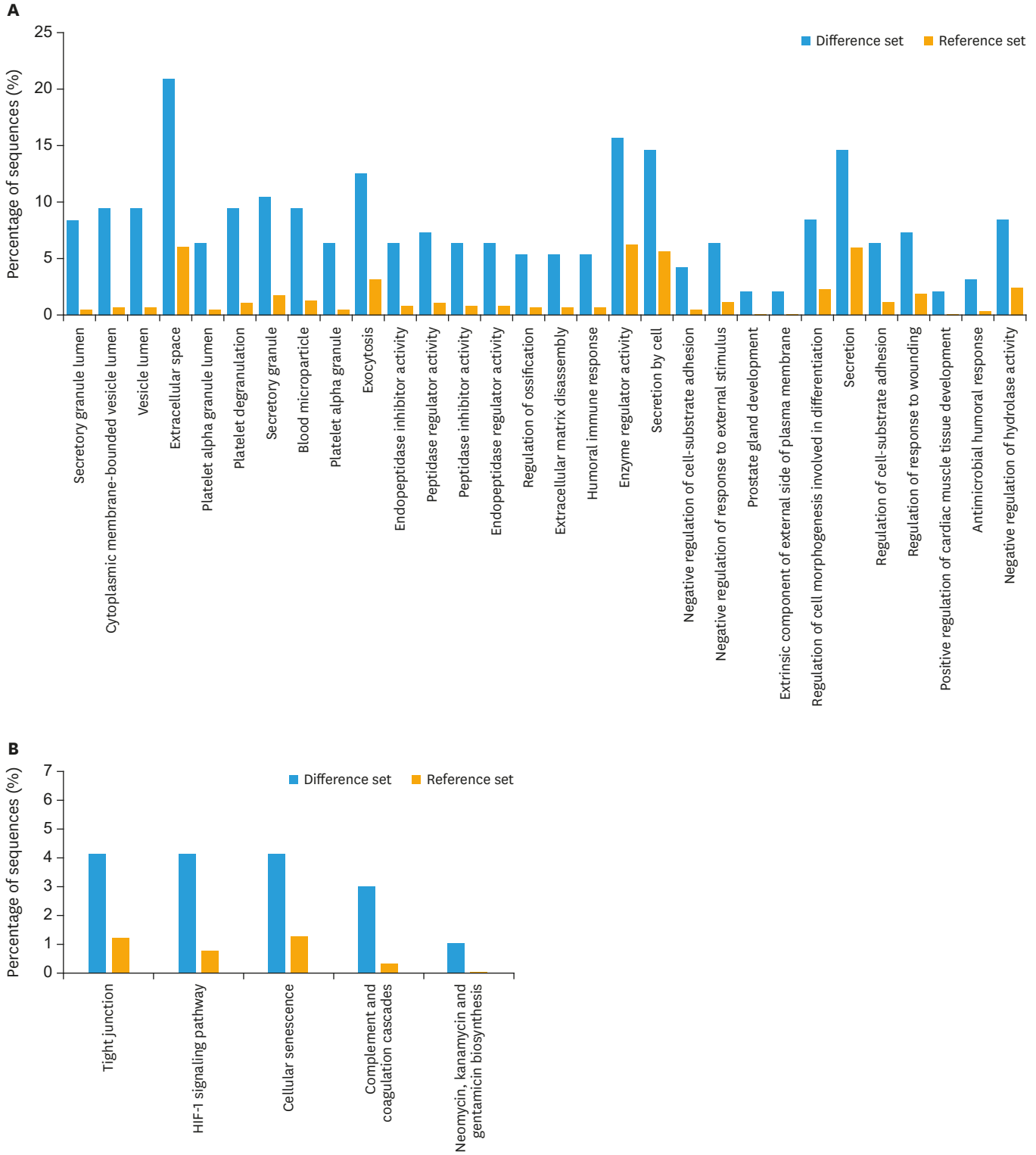

Fig. 3. GO and KEGG analysis in carboplatin group. **(**A) GO enrichment analysis between the carboplatin and mock groups; (B) KEGG pathway analysis between the carboplatin and mock groups.
GO, Gene Ontology; KEGG, Kyoto Encyclopedia of Genes and Genomes.

https://doi.org/10.3802/jgo.2020.31.e28

paclitaxel group and 3 of the proteins upregulated in the carboplatin group have previously been associated with chemoresistance, including the APOA1 protein which exhibited the most significant differences in both paclitaxel and carboplatin chemoresistance and which we chose to verify (**Supplementary Table 2**).

5. Screening and verification of proteins related to drug resistance

According to previous studies and the results of the GO and KEGG pathway analyses, APOA1 was the most significantly upregulated protein in both paclitaxel- and carboplatin-chemoresistant cells; therefore, we selected APOA1 as the target protein for gene overexpression experiments. A non-fluorescent lentivirus for the overexpression of APOA1 was constructed and co-cultured with SiHa cells. All cells were in good condition and the efficiency of infection was qualified. APOA1 overexpression in the SiHa cells was detected by RT-PCR and WB. APOA1 gene expression in the overexpression group was 355.459-fold higher than that in negative control group, whilst APOA1 protein expression in the overexpression group was higher than that in negative control group (**Fig. 4**). The concentrations of paclitaxel and carboplatin in the APOA1 overexpression group were assessed using the CCK-8 assay. The IC_{50} of paclitaxel in the APOA1 overexpression group was higher (0.01082 μg/mL) than that of the negative control group (0.008976 μg/mL); however, the difference between the IC_{50} of paclitaxel in the APOA1 overexpression and negative control groups was not significant. The IC_{50} of carboplatin in the APOA1 overexpression group was higher (86.31 μg/mL) than that of the negative control group (51.88 μg/mL); however, the difference between the IC_{50} of carboplatin in the APOA1 overexpression and negative control groups was not significant (**Fig. 5**).

6. High APOA1 protein expression in drug-resistant squamous cell cervical cancer tissues verified by IHC

Ten cases of cervical squamous cell carcinoma presented with locally advanced squamous cell cervical cancer. These patients were also being treated with platinum-based combined paclitaxel NACT prior to primary surgical intervention. Clinical remission was evaluated according to RECIST, the patients with SD and PD are defined as chemotherapy-resistant and the patients with CR are classified as chemotherapy-sensitive. IHC revealed cytoplasmic APOA1 expression in the squamous cell carcinoma tissues of 40% (2/5) of the patients in the chemotherapy-resistant (carboplatin- and paclitaxel-resistant) group and only 20% (1/5) of the patients in the chemotherapy-sensitive group. The average staining intensity score was 6±1.67 in both the chemotherapy-resistant and chemotherapy-sensitive groups (**Table 1**).

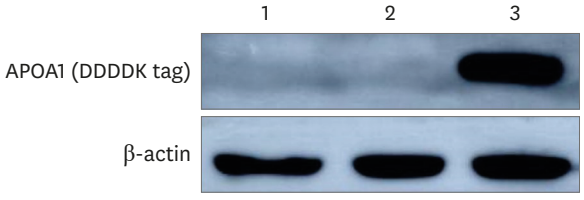

Fig. 4. Western blot demonstrating over-expression of APOA1 in SiHa cells. A non-fluorescent lentivirus for the overexpression of APOA1 was constructed and co-cultured with SiHa cells. APOA1 overexpression was detected in the SiHa cells by western blotting. APOA1 protein (DDDDK tag) expression was higher in the overexpression group than in the negative control group.
1, SiHa cell; 2, negative control group (empty lentivirus); 3, over-expression of APOA1 SiHa cell.

https://doi.org/10.3802/jgo.2020.31.e28

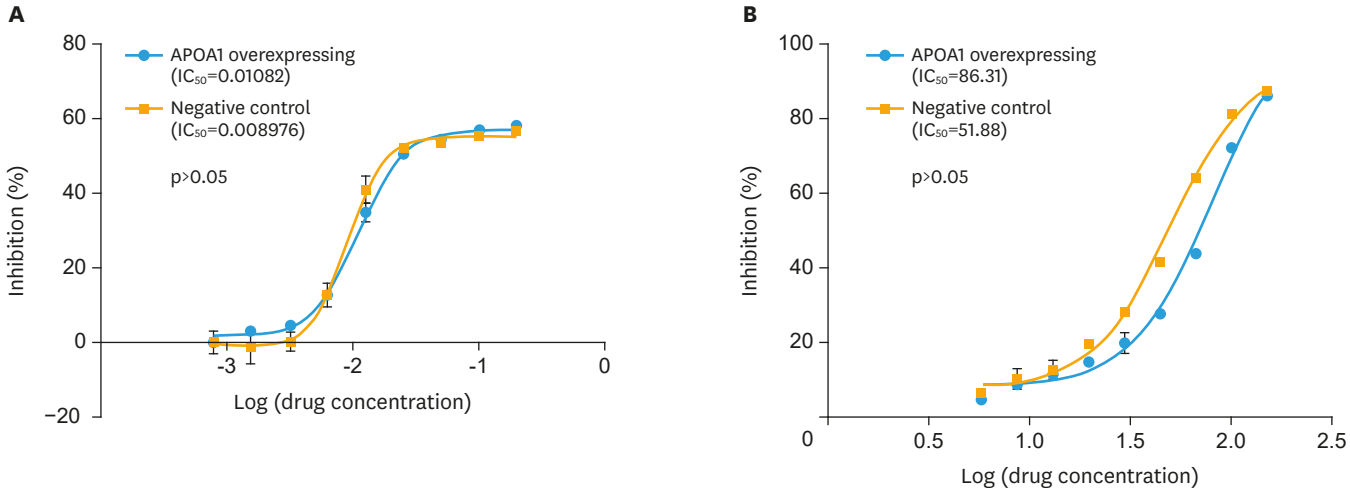

Fig. 5. IC_{50} of paclitaxel and carboplatin in lentivirus infected SiHa cells. (A) The IC_{50} of paclitaxel in the APOA1 overexpression group and negative control group ($p>0.05$); (B) The IC_{50} of carboplatin in the APOA1 overexpression group and negative control group ($p>0.05$).
IC_{50}, half-maximal inhibitory concentration.

Table 1. Expreesion of APOA1 proteins was verified by immunohistochemistry

Sample	High expression	Low expression	Total
Chemotherapy-resistant group	40.0% (2/5)	60.0% (3/5)	5
Chemotherapy-sensitive group	20.0% (1/5)	80.0% (4/5)	5
Mean±standard deviation (score)	6±1.67	6±1.67	-

DISCUSSION

NACT is useful in the control of LACC, with early or pre-chemotherapy NACT used to reduce tumor volume prior to surgery or radiotherapy. The paclitaxel/carboplatin combination is now the preferred NACT regimen, with preliminary data indicating that high-dose regimens are feasible and effective (overall response rate: 67.8%–87%) [11]. Because the efficacy of chemotherapy on cervical squamous cell carcinoma varies from person to person, identifying differentially expressed proteins related to paclitaxel/carboplatin resistance could provide a basis for future studies on drug-resistance pathways.

APOA1 is a major protein component of high-density lipoprotein (HDL) in plasma, an anti-atherogenic factor in lipid metabolism [12], and is synthesized mainly in the liver and small intestine [13]. Several studies have shown that APOA1 can suppress inflammation, tumor growth, angiogenesis, invasion, and metastasis [14], whilst many proteomics-based studies have shown that APOA1 is a biomarker for many types of cancer, including breast, ovarian, and gastric cancers as well as pancreatic carcinomas [14-22]. The role of APOA1 in cancer pathophysiology is thought to be related to its phospholipid binding ability; for example, lysophospholipids have been shown to play a critical role in cancer development and have been reported to be major biomarkers for various cancers [23,24]. Many studies have focused on the associations between HDL and APOA1, lipid profiles, and cancer risk, suggesting that low HDL and APOA1 levels and increased lipid ratios are inversely associated with an increased risk of various cancers [18,22]. Animal studies have shown that APOA1 gene overexpression can inhibit tumor growth in mice and prolong survival [25]; however, until now no studies have examined the effect of APOA1 on chemoresistance. In this study, we used qPCR to verify that APOA1 upregulation can increase paclitaxel and carboplatin

https://doi.org/10.3802/jgo.2020.31.e28

resistance. The IC_{50} values of paclitaxel and carboplatin were nearly 1.2-fold and 1.5-fold higher, respectively, in the APOA1-overexpressing SiHa cells than in the normal SiHa cells. IHC showed that APOA1 was highly expressed in the paclitaxel- and carboplatin- resistant squamous cell carcinomas of cervical tissues than in the paclitaxel- and carboplatin-sensitive group; however, the mechanism of the chemoresistance remains unknown. According to recent studies [26], APOA1 chemoresistance may be related to anti-apoptotic and antioxidant functions and the transport of other antioxidants, thus may directly affect intracellular signaling pathways. Further experiments are required to clarify the mechanism of APOA1 chemoresistance.

The iTRAQ is based on the high sensitivity of mass spectrometry; it has a low limit of detection, fast analysis time, remarkable separation, and is highly automated. Ding et al. [27] used iTRAQ labeling and Nano LC-MS/MS analysis to detect differentially expressed proteins in cervical cancer, gaining a systematic insight into the proteins participating in cervical tumor oncogenesis and improving current target therapies. They identified 3,647 proteins, among which 294 had distinct expression levels in cervical cancer samples compared to the paired non-tumor samples. Furthermore, the study suggested that suppressing G6PD expression may be a promising strategy for developing novel therapeutic drugs against cancer. Using iTRAQ, Xie et al. [28] determined the protein expression profiles of the epididymal luminal fluids in infertile and normal rats, validating the proteome data by enzyme-linked immunosorbent assays. The authors tested 1,045 proteins, 23 of which presented different expression profiles in the infertile and normal rats (7 downregulated and 16 upregulated). Of the 7 proteins significantly downregulated by dutasteride in the epididymal luminal fluids, 3 were β-defensins (Defb2, Defb18, and Defb39), which may therefore be key proteins in epididymal sperm maturation and male fertility. The results provided new epididymal targets for male contraception and infertility therapy. Using an iTRAQ-based quantitative proteomic approach, Wu et al. [29] detected chemotherapy-induced responses at the protein and metabolite levels by searching for novel plasma markers to predict platinum-based chemotherapy resistance in EOC patients and thus improve clinical response rates. They identified 248 proteins from 2 independent experiments, among which fibronectin 1 (FN1), serpin family A member 1 (SERPINA1), glutathione peroxidase 3 (GPX3), and orosomucoid 1 (ORM1) were validated by western blot analysis and enzyme-linked immunosorbent assay. Platinum resistance, which is likely associated with differentially expressed proteins, as well as FN1, SERPINA1, and ORM1 may play positive roles in chemotherapy. Therefore, these types of studies could provide biomarkers for predicting chemotherapeutic response, reverse drug resistance, or even lead to novel targets for therapeutic intervention.

In this study, iTRAQ was used to identify 7,139 differentially expressed proteins related to NACT in SiHa cells, and biomarkers with MWs of 1,000–50,000 Da were successfully evaluated. A comparative analysis of the differentially expressed proteins between the paclitaxel, carboplatin, and mock groups was performed according to the following screening criteria: upregulated more than 1.2-fold or downregulated less than 0.83-fold in the 3 groups ($p<0.05$). Combined with the results of previous reports, 53 differentially expressed proteins were identified in the paclitaxel vs mock group, and 85 were identified in the carboplatin vs mock group. The differentially expressed proteins were screened by GO and KEGG pathway analyses as candidate drug-resistance markers, including the 43 and 70 proteins upregulated in the paclitaxel vs. mock and carboplatin vs. mock groups, respectively. VTN [30], PTSG [31], CLU [15], HLA [16], and NORTCH [17] were detected by iTRAQ, and have been

https://doi.org/10.3802/jgo.2020.31.e28

previously reported to be related to chemoresistance. Overall, iTRAQ is a reliable method for exploring the factors affecting chemoresistance at the protein level.

ACKNOWLEDGMENTS

We are grateful to all the reviewers and editors who provided comments that substantially improved the manuscript.

SUPPLEMENTARY MATERIALS

Supplementary Table 1

Protein identification results

Click here to view

Supplementary Table 1

Upregulated proteins related to chemotherapy resistance in the paclitaxel/carboplatin group

Click here to view

REFERENCES

1. Torre LA, Bray F, Siegel RL, Ferlay J, Lortet-Tieulent J, Jemal A. Global cancer statistics, 2012. CA Cancer J Clin 2015;65:87-108.
PUBMED | CROSSREF
2. Moore MA, Attasara P, Khuhaprema T, Le TN, Nguyen TH, Raingsey PP, et al. Cancer epidemiology in mainland South-East Asia - past, present and future. Asian Pac J Cancer Prev 2010;11 Suppl 2:67-80.
PUBMED
3. Chemoradiotherapy for Cervical Cancer Meta-Analysis Collaboration. Reducing uncertainties about the effects of chemoradiotherapy for cervical cancer: a systematic review and meta-analysis of individual patient data from 18 randomized trials. J Clin Oncol 2008;26:5802-12.
PUBMED | CROSSREF
4. Eifel PJ, Winter K, Morris M, Levenback C, Grigsby PW, Cooper J, et al. Pelvic irradiation with concurrent chemotherapy versus pelvic and para-aortic irradiation for high-risk cervical cancer: an update of radiation therapy oncology group trial (RTOG) 90-01. J Clin Oncol 2004;22:872-80.
PUBMED | CROSSREF
5. McCormack M, Kadalayil L, Hackshaw A, Hall-Craggs MA, Symonds RP, Warwick V, et al. A phase II study of weekly neoadjuvant chemotherapy followed by radical chemoradiation for locally advanced cervical cancer. Br J Cancer 2013;108:2464-9.
PUBMED | CROSSREF
6. Wang Y, Wang G, Wei LH, Huang LH, Wang JL, Wang SJ, et al. Neoadjuvant chemotherapy for locally advanced cervical cancer reduces surgical risks and lymph-vascular space involvement. Chin J Cancer 2011;30:645-54.
PUBMED | CROSSREF
7. Yang Z, Chen D, Zhang J, Yao D, Gao K, Wang H, et al. The efficacy and safety of neoadjuvant chemotherapy in the treatment of locally advanced cervical cancer: a randomized multicenter study. Gynecol Oncol 2016;141:231-9.
PUBMED | CROSSREF
8. Lawson D, Arensburger P, Atkinson P, Besansky NJ, Bruggner RV, Butler R, et al. VectorBase: a data resource for invertebrate vector genomics. Nucleic Acids Res 2009;37:D583-7.
PUBMED | CROSSREF

9. Mallmann P, Mallmann C. Neoadjuvant and adjuvant chemotherapy of cervical cancer. Oncol Res Treat 2016;39:522-4.
PUBMED | CROSSREF
10. Eisenhauer EA, Therasse P, Bogaerts J, Schwartz LH, Sargent D, Ford R, et al. New response evaluation criteria in solid tumours: revised RECIST guideline (version 1.1). Eur J Cancer 2009;45:228-47.
PUBMED | CROSSREF
11. Lapresa M, Parma G, Portuesi R, Colombo N. Neoadjuvant chemotherapy in cervical cancer: an update. Expert Rev Anticancer Ther 2015;15:1171-81.
PUBMED | CROSSREF
12. Bencharif K, Hoareau L, Murumalla RK, Tarnus E, Tallet F, Clerc RG, et al. Effect of apoA-I on cholesterol release and apoE secretion in human mature adipocytes. Lipids Health Dis 2010;9:75.
PUBMED | CROSSREF
13. Jahangiri A. High-density lipoprotein and the acute phase response. Curr Opin Endocrinol Diabetes Obes 2010;17:156-60.
PUBMED | CROSSREF
14. Moore LE, Fung ET, McGuire M, Rabkin CC, Molinaro A, Wang Z, et al. Evaluation of apolipoprotein A1 and posttranslationally modified forms of transthyretin as biomarkers for ovarian cancer detection in an independent study population. Cancer Epidemiol Biomarkers Prev 2006;15:1641-6.
PUBMED | CROSSREF
15. Magadoux L, Isambert N, Plenchette S, Jeannin JF, Laurens V. Emerging targets to monitor and overcome docetaxel resistance in castration resistant prostate cancer (review). Int J Oncol 2014;45:919-28.
PUBMED | CROSSREF
16. Zhang ZJ, Bulur PA, Dogan A, Gastineau DA, Dietz AB, Lin Y. Immune independent crosstalk between lymphoma and myeloid suppressor CD14^{+}HLA-DR$^{low/neg}$ monocytes mediates chemotherapy resistance. Oncoimmunology 2015;4:e996470.
PUBMED | CROSSREF
17. Ding Y, Shen Y. Notch increased vitronection adhesion protects myeloma cells from drug induced apoptosis. Biochem Biophys Res Commun 2015;467:717-22.
PUBMED | CROSSREF
18. Guo X, Hao Y, Kamilijiang M, Hasimu A, Yuan J, Wu G, et al. Potential predictive plasma biomarkers for cervical cancer by 2D-DIGE proteomics and ingenuity pathway analysis. Tumour Biol 2015;36:1711-20.
PUBMED | CROSSREF
19. Liu X, Zheng W, Wang W, Shen H, Liu L, Lou W, et al. A new panel of pancreatic cancer biomarkers discovered using a mass spectrometry-based pipeline. Br J Cancer 2017;117:1846-54.
PUBMED | CROSSREF
20. Lozano-Pope I, Sharma A, Matthias M, Doran KS, Obonyo M. Effect of myeloid differentiation primary response gene 88 on expression profiles of genes during the development and progression of Helicobacter-induced gastric cancer. BMC Cancer 2017;17:133.
PUBMED | CROSSREF
21. Nosov V, Su F, Amneus M, Birrer M, Robins T, Kotlerman J, et al. Validation of serum biomarkers for detection of early-stage ovarian cancer. Am J Obstet Gynecol 2009;200:639.e1-5.
PUBMED | CROSSREF
22. Cine N, Baykal AT, Sunnetci D, Canturk Z, Serhatli M, Savli H. Identification of ApoA1, HPX and POTEE genes by omic analysis in breast cancer. Oncol Rep 2014;32:1078-86.
PUBMED | CROSSREF
23. Lv GM, Li P, Wang WD, Wang SK, Chen JF, Gong YL. Lysophosphatidic acid (LPA) and endothelial differentiation gene (Edg) receptors in human pancreatic cancer. J Surg Oncol 2011;104:685-91.
PUBMED | CROSSREF
24. Panupinthu N, Lee HY, Mills GB. Lysophosphatidic acid production and action: critical new players in breast cancer initiation and progression. Br J Cancer 2010;102:941-6.
PUBMED | CROSSREF
25. Zamanian-Daryoush M, Lindner D, Tallant TC, Wang Z, Buffa J, Klipfell E, et al. The cardioprotective protein apolipoprotein A1 promotes potent anti-tumorigenic effects. J Biol Chem 2013;288:21237-52.
PUBMED | CROSSREF
26. Hyka N, Dayer JM, Modoux C, Kohno T, Edwards CK 3rd, Roux-Lombard P, et al. Apolipoprotein A-I inhibits the production of interleukin-1β and tumor necrosis factor-α by blocking contact-mediated activation of monocytes by T lymphocytes. Blood 2001;97:2381-9.
PUBMED | CROSSREF

27. Ding Y, Yang M, She S, Min H, Xv X, Ran X, et al. iTRAQ-based quantitative proteomic analysis of cervical cancer. Int J Oncol 2015;46:1748-58.
PUBMED | CROSSREF

28. Xie SW, Li GT, Qu LJ, Cao Y, Wang Q, Zhou JY, et al. Identification of new epididymal luminal fluid proteins involved in sperm maturation in infertile rats treated by dutasteride using iTRAQ. Molecules 2016;21:E602.
PUBMED | CROSSREF

29. Wu W, Wang Q, Yin F, Yang Z, Zhang W, Gabra H, et al. Identification of proteomic and metabolic signatures associated with chemoresistance of human epithelial ovarian cancer. Int J Oncol 2016;49:1651-65.
PUBMED | CROSSREF

30. Lee YS, Ryu SW, Bae SJ, Park TH, Kwon K, Noh YH, et al. Cross-platform meta-analysis of multiple gene expression profiles identifies novel expression signatures in acquired anthracycline-resistant breast cancer. Oncol Rep 2015;33:1985-93.
PUBMED | CROSSREF

31. Choi CH, Kang G, Min YD. Reversal of P-glycoprotein-mediated multidrug resistance by protopanaxatriol ginsenosides from Korean red ginseng. Planta Med 2003;69:235-40.
PUBMED | CROSSREF